ELSEVIER

Contents lists available at ScienceDirect

# **Chemical Physics Letters**

journal homepage: www.elsevier.com/locate/cplett



#### Research paper

# Carbon isotope effects in the artificial photosynthesis reactions catalyzed by nanostructured Co/CoO



Ming Zeng<sup>a</sup>, Zhe Kan<sup>b</sup>, Zibo Wang<sup>a</sup>, Mengyan Shen<sup>a,b,\*</sup>

- <sup>a</sup> Department of Physics and Applied Physics, University of Massachusetts Lowell, One University Avenue, Lowell, MA 01854, USA
- <sup>b</sup> Nanomanufacturing Center, University of Massachusetts Lowell, One University Avenue, Lowell, MA 01854, USA

#### HIGHLIGHTS

- Carbon isotope effects have been observed in artificial photosynthesis.
- The dissociation of <sup>12</sup>CO<sub>2</sub> is easier than that of <sup>13</sup>CO<sub>2</sub>.
- The same carbon isotope atoms have a relatively higher probability to bond together to form hydrocarbon chains.
- The quantum mechanics tunneling of electrons explains the carbon isotope effects.

#### ARTICLE INFO

# Keywords:

A. Isotope effect

B. Carbon dioxide

D. Artificial photosynthesis

#### ABSTRACT

Although carbon dioxide  $(CO_2)$  and water  $(H_2O)$  have been converted into hydrocarbons, ranging from pentane  $(C_5H_{12})$  to octadecane  $(C_{18}H_{38})$  through an artificial photosynthesis reaction catalyzed by nanostructured CO/COO, the mechanism of the reaction is not very clear. In this work, the isotope effect of carbon is studied by conducting the  $^{13}C/^{12}C$  competition experiments using an equal molar ratio of  $^{13}CO_2$  and  $^{12}CO_2$  as the reagents. It is shown that the dissociation of  $^{12}CO_2$  is easier than that of  $^{13}CO_2$ , and the same carbon isotope atoms have a relatively higher probability to bond together to form the hydrocarbon chains. The quantum mechanical analysis of the observed isotope effect helps us to better understand the mechanism for hydrocarbon synthesis.

## 1. Introduction

Artificial photosynthesis, the analog of the natural process of photosynthesis (converting carbon dioxide and water into carbohydrates or hydrocarbons), has attracted wide interest because it stores solar energy as chemical energy while consuming greenhouse gas [1]. Researchers have devoted a great deal of effort to develop a direct process to generate hydrocarbon fuels from  ${\rm CO_2}$  and water. This is desirable because it consumes CO2, one of the main greenhouse gases, and also produces useable liquid hydrocarbon fuels. In 2009, long-chain hydrocarbons were synthesized from CO2 and water with laser-induced nanostructured cobalt (Co) catalyst at lower temperature and pressure than in previous works [2-5]. By following the same laser irradiation fabrication methods, novel nanostructured materials with special electronic, thermal, and catalytic properties were reported recently [6-8]. A mechanism of surface plasmon excitation focusing was proposed, where the intensity of the sunlight is greatly enhanced around the tips of the Co nanostructures. The enhanced photons dissociate the CO2 and water

molecules, and CO and  $\rm H_2$  molecules associate to form hydrocarbons [2–5]. Recently, the long-chain hydrocarbon synthesis has been further studied with a low-cost nanostructured Co catalyst made using an acidetching method. The adsorption of the  $\rm CO_2$  molecules on the surface of the catalyst was found to act as a source of carbon, and the fact that the lowest unoccupied molecular orbital (LUMO) of the adsorbed  $\rm CO_2$  was also found to be near to the bottom of the conduction band of  $\rm CoO$  which plays an important role in the dissociation of  $\rm CO_2$  [9]. However, the dynamics of the dissociation of  $\rm CO_2$  and the hydrocarbon synthesis is not understood. We use carbon isotopes to confirm the hydrocarbon synthesis mechanics and to investigate the dynamics as well.

In this work, we performed a series of  $^{13}\text{C}/^{12}\text{C}$  competition experiments to study the carbon isotope effects. The kinetic isotope effect is the change in the rate of a chemical reaction when one of the atoms in the reactants is substituted with one of its isotopes [10]. It is a powerful tool for studying reaction mechanisms and functions, which has been studied both theoretically and experimentally [11–15]. In this paper, we have conducted the  $^{13}\text{C}/^{12}\text{C}$  competition experiments using an equal

<sup>\*</sup> Corresponding author at: Department of Physics and Applied Physics, University of Massachusetts Lowell, One University Avenue, Lowell, MA 01854, USA. E-mail address: Mengyan\_Shen@uml.edu (M. Shen).

Chemical Physics Letters 754 (2020) 137731

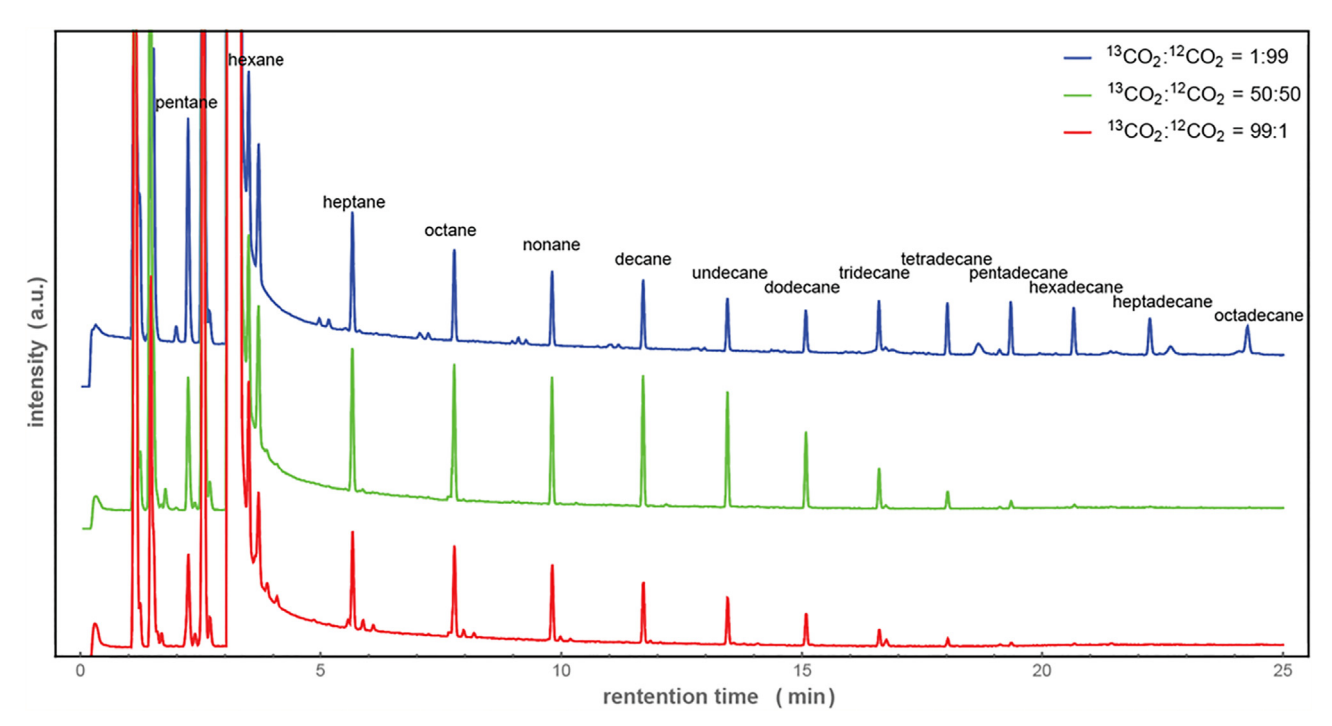


Fig. 1. Gas chromatography (GC) spectra of hydrocarbons produced with carbon dioxide at ratios of <sup>13</sup>C/<sup>12</sup>C: (a) 1:99, (b) 50:50 and (c) 99:1 after 20 h of light irradiation.

molar ratio of  $^{13}\text{CO}_2$  and  $^{12}\text{CO}_2$  as the reagents to confirm whether there is a carbon isotope effect in this nanostructured Co/CoO-catalyzed CO<sub>2</sub> and water conversion reaction. It is shown that  $^{12}\text{CO}_2$  dissociates easier than  $^{13}\text{CO}_2$ . The distribution derived from a classical mechanics model that assumes hydrocarbons are randomly formed without an isotope effect is inconsistent with experiments. Using the quantum mechanical concept of resonant tunneling and applying Bayesian statistics, we study the tendency that the same carbon isotope atoms have a relatively higher probability to bond together to form the hydrocarbon chains. With the concept of quantum mechanics, the observed isotope effects can be explained and helps us better understand the mechanism of the hydrocarbon synthesis from carbon dioxide and water at the comparatively low temperature and pressure [2–5].

# 2. Experimental

# 2.1. Reagents and catalyst

The cobalt (Co) powder was obtained from Goodfellow. The diameters of the Co micro-particles are in the range of 50–100  $\mu m$ . The Co micro-particles were mixed with a 3.5% aqueous solution of hydrogen chloride (HCl) for 10 min, then rinsed with distilled water. The oxide layered structures were removed from the Co particle surfaces by acid etching. The catalyst was then degassed in vacuum for approximately 1 h to remove the carbon dioxide adsorbed on the surfaces. Nanoflakes were then formed on the particle surfaces after placing the Co powder in air at room temperature for 2 h. This method was reported in a previous article [9]. In this work, we used carbon dioxide (CO<sub>2</sub>) isotope mixtures with three different ratios of  $^{13}\text{CO}_2/^{12}\text{CO}_2$ : 1:99 (naturally abundant), 50:50, and 99:1 (purchased from Sigma-Aldrich Corporation).

#### 2.2. Artificial photosynthesis of carbon dioxide and water procedure

2-g catalyst was loaded in a glass reactor (20 mL), and 350 mg of distilled water was added into the reactor to cover the catalyst. Afterwards, the reactor was evacuated to about  $1\times 10^{-3}$  atm and then

filled with  $^{13}\text{CO}_2/^{12}\text{CO}_2$  mixtures of different ratios (a) 1:99, (b) 50:50, and (c) 99:1 to an absolute pressure of 2 atm at room temperature. A solar lamp for simulating natural sunlight (Honle, SOL 500) with a power density of  $100~\text{mW/cm}^2$  was used to irradiate the nanostructured Co micro-particles in the sealed reactor at a temperature of  $\sim 110~^\circ\text{C}$ . After an irradiation period of 20 h, the reactor was cooled to room temperature.

# 2.3. Product analysis

Approximately 3 mL of dichloromethane (DCM) was injected into the reactor to extract non-volatile organic products. The DCM extract was then analyzed using a Bruker Scion SQ gas chromatography-mass spectrometry (GC-MS) with a 30 m ZB-624 capillary column. To qualify the GC-MS apparatus used in this experiment, 0.1 mL of standard <sup>12</sup>CH<sub>3</sub>OH (from Sigma) and 0.1 mL of standard <sup>13</sup>CH<sub>3</sub>OH (99 atom % <sup>13</sup>C, from Aldrich) were separately dissolved in 1 mL of dichloromethane (CH<sub>2</sub>Cl<sub>2</sub>). The mixtures were then analyzed by GC-MS. We did not notice any difference between their MS intensities, but their MS peaks shift corresponding to the mass difference between 12C and  $^{13}\text{C}$  [8]. Standard natural abundance alkanes from  $\text{C}_8\text{H}_{18}$  to  $\text{C}_{20}\text{H}_{42}$ were purchased from Sigma. The full molecule MS intensity of the standard natural abundance hydrocarbons measured with the GC-MS apparatus yielded a the ratio  ${}^{13}C$ :  ${}^{12}C = 1.10\%$ , which is close to the natural isotopic ratio of 1.109% [16,17]. The GC-MS apparatus is almost equally sensitive to <sup>13</sup>C and <sup>12</sup>C within a precision about 0.1% [9]. The relative intensities of the peaks of full molecule MS provide us a direct measure of the relative abundance of the isotopes in the hydrocarbons [18,19]. Therefore, the relative abundance of the isotopes can be determined from the relative abundance of the molecular ions M + i[18.19]; where i represents the number of the  $^{13}$ C atoms incorporated into the produced hydrocarbon molecules. Therefore, the <sup>13</sup>C/<sup>12</sup>C ratio in a hydrocarbon chain with a carbon number of n can be calculated by

$$\frac{^{13}C}{^{12}C} = \frac{\sum_{i=0}^{i=n} A_{M+i} \cdot i}{\sum_{i=0}^{i=n} A_{M+i} \cdot (n-i)}$$
(1)

where  $A_{M+i}$  is the relative intensity of the M+i peak of an alkane.

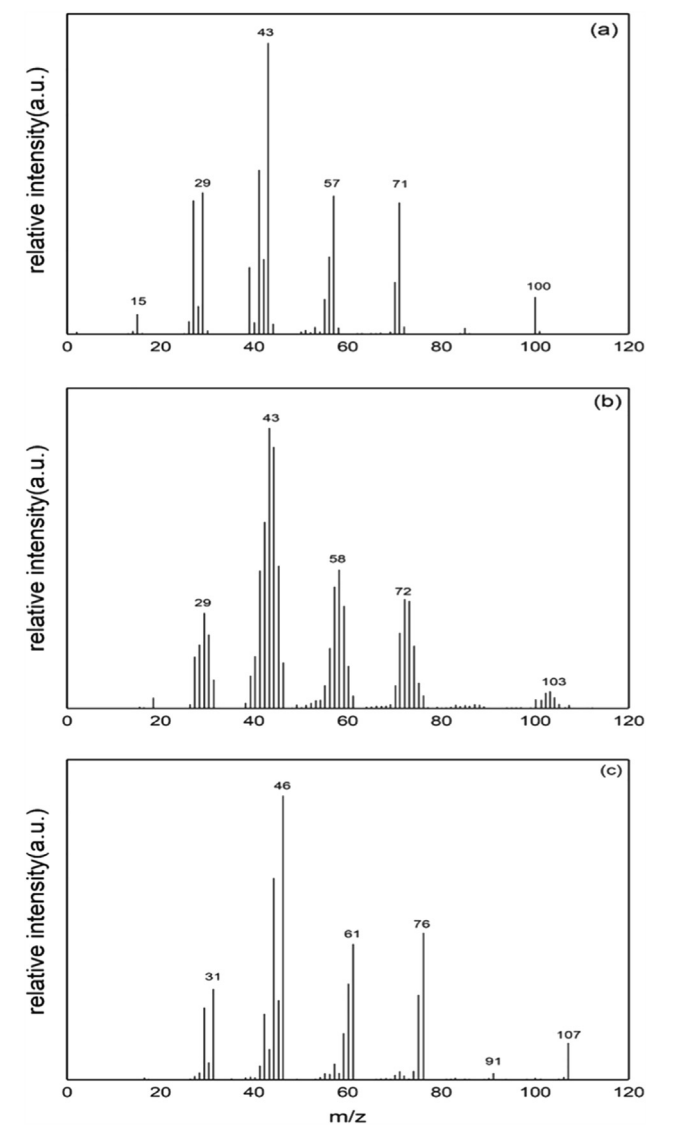


**Fig. 2.** Mass spectra of the heptane ( $C_7H_{16}$ ) produced with carbon dioxide at ratios of  $^{13}CO_2/^{12}CO_2$ : (a) 1:99, (b) 50:50 and (c) 99:1 after 20 h of light irradiation.

#### 3. Results and discussion

Fig. 1 shows the gas chromatography (GC) spectra of samples produced with carbon dioxide at ratios of  $^{13}\text{C}/^{12}\text{C}$ : (a) 1:99, (b) 50:50, and (c) 99:1 after 20 h of light irradiation. The spectrum in blue for experiment (a) reveals a series of straight-chain hydrocarbon compounds ranging from propane (C $_3\text{H}_8$ ) to octadecane (C $_1\text{B}\text{H}_3\text{B}$ ). This is three carbons longer than that from previous detected results [9]. In the green and red spectra (experiments (b) and (c), respectively), the longest observed hydrocarbons are shorter than that in the blue spectrum for experiment (a).

# 3.1. The carbon isotope effect in nanostructured Co/CoO catalyzed ${\rm CO_2}$ and water conversion reaction

Fig. 2 shows the comparison of the mass spectra of the heptane  $(C_7H_{16})$  obtained from experiments (a), (b) and (c). It demonstrates that  $^{13}$ C is incorporated into the produced alkanes. Other hydrocarbons show similar results. Fig. 3 zooms into the spectra in Fig. 2, and onto the molecular peaks of the heptane  $(C_7H_{16})$  synthesized from experiments (a), (b) and (c). The ion peak is analyzed to calculate the ratio of

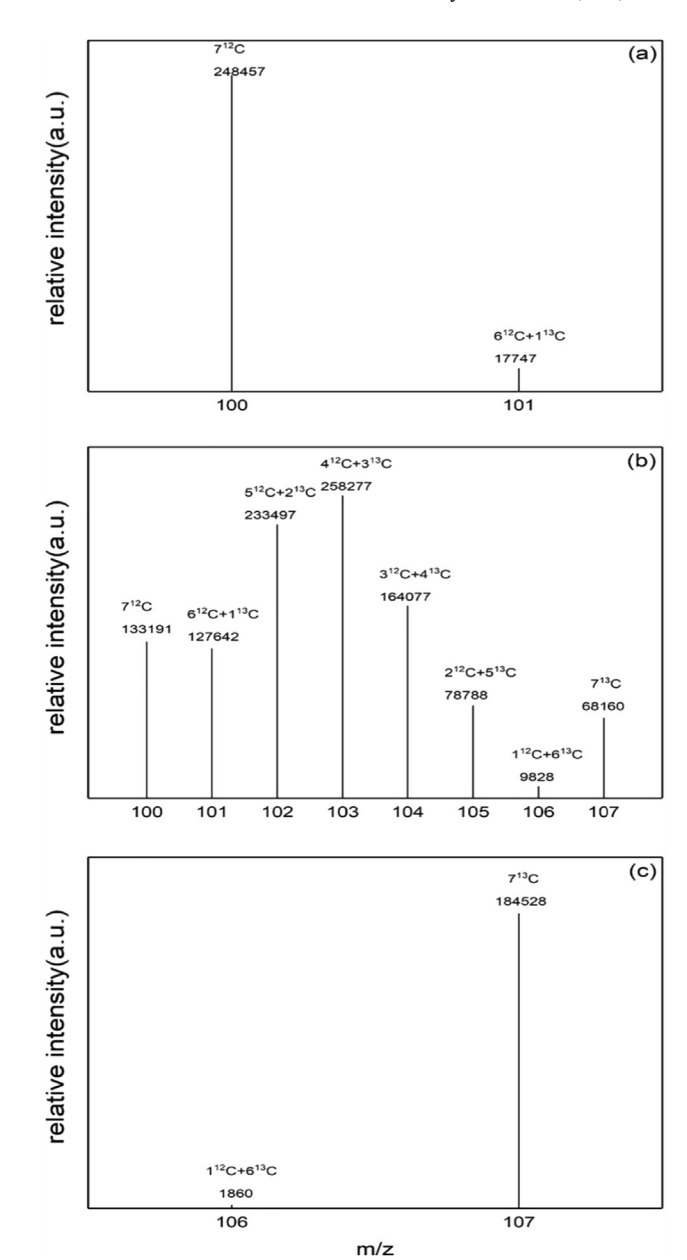


Fig. 3. The molecular ion peaks of the heptane  $(C_7H_{16})$  synthesized from experiments (a), (b) and (c).

 $^{13}$ C to  $^{12}$ C. The intensity of each peak (from M to M + 7) is proportional to the abundance of the molecule in the sample [18]. The molecular ion peak at m/z=100 corresponds to  $C_7H_{16}$  with all 7 carbon atoms being  $^{12}$ C. The peak at m/z=101 corresponds to 1 of the 7 carbon atoms being replaced by  $^{13}$ C; the peak at m/z=102 corresponds to 2 of the 7 carbon atoms being replaced by  $^{13}$ C; and so on; the peak at m/z=107 corresponds to the 7 carbon atoms being  $^{13}$ C. The ratio of  $^{13}$ C to  $^{12}$ C is calculated to be 0.65, using Eq. (1) for experiment (b). The analysis of the ratio of  $^{13}$ C to  $^{12}$ C ratio in other hydrocarbons for experiments (a), (b) and (c) are listed in Table 1.

The results of (a) agree with the fact that the natural abundance of Carbon-13 is 1.109% [17] while for experiment (c), the carbon-12 related molecular MS signal is too weak in the GC spectra of hydrocarbons with carbon numbers larger than 7 to conclude reliable ratio of  $^{13}\mathrm{C}$  to  $^{12}\mathrm{C}$ . This anomalous phenomenon is explained in Section 3.3 using quantum mechanics. There is a carbon isotope effect in experiment (b): we have more  $^{12}\mathrm{C}$  atoms than  $^{13}\mathrm{C}$  atoms in the hydrocarbons, as the ratio of  $^{13}\mathrm{C}$  to  $^{12}\mathrm{C}$  is 0.65, i.e. the dissociation of  $^{12}\mathrm{CO}_2$  is easier

Table 1 Quantitative analysis of the  $^{13}$ C to  $^{12}$ C ratio for experiment (a), (b) and (c).

	(a)	(b)	(c)
C <sub>7</sub> H <sub>16</sub>	0.01	0.65	700
$C_8H_{18}$	0.01	0.65	N/A
$C_9H_{20}$	0.01	0.66	N/A
$C_{10}H_{22}$	0.01	0.65	N/A
$C_{11}H_{24}$	0.01	0.69	N/A
$C_{12}H_{26}$	0.01	0.62	N/A

than that of 13CO2

#### 3.2. Estimation of the isotope effect in the dissociation of CO<sub>2</sub>

In the artificial photosynthesis reaction catalyzed by nanostructured Co/CoO, CO<sub>2</sub> molecules may attach to the CoO surface that encloses a Co nanostructure. There are some defect energy levels in the band gap of CoO at the interface between CoO and Co [9,10]. When sunlight irradiates the nanostructured surface, electrons may be excited from a defect energy level to the conduction band of CoO and then quantum tunnel to the LUMO of the  $\rm CO_2$  molecules through the plasmonic nanofocusing at the interface [8,9]. On the other hand, the plasmon-induced hot-electrons in Co may also inject into the conduction band of CoO and then quantum tunnel to the LUMO energy levels of  $\rm CO_2$  molecules [8,9]. Then the  $\rm CO_2$  molecules will dissociate because the charged  $\rm CO_2$  molecules are not stable. The dissociated molecules will form hydrocarbons on the surface of Co nanostructures [20–22].

Because of the chemisorption of  $CO_2$  onto the CoO, their electrons are in the same system [9]. The potential energy of an electron close to the surface outside a solid is higher than that at a distant location [23,24], while the electron near a  $CO_2$  molecule absorbed onto the solid surface is localized around the molecule. Considering these effects, we illustrate the electron potential energy V(r) of a  $CO_2$  molecule absorbed onto the CoO surface with the LUMO near the bottom of the conduction band of CoO in Fig. 4. The excited electrons resonantly tunnel to the  $CO_2$ 's LUMO levels with vibrational energies. The mass of  $CO_2$  is larger than that of  $CO_2$ . Hence, the LUMO of  $CO_2$  is lower than that of  $CO_2$ . A previous study in reference [25] showed that  $CO_2$  and  $CO_3$  have different ground state energies when they are adsorbed onto  $CO_2$  with bonding energies:  $CO_2$  = 0.25 eV and  $CO_2$  = 0.26 eV. Instead of using the potential  $CO_2$  shown in Fig. 4, we can use a two-step potential barrier to simply estimate the tunneling:

$$V(r) = \begin{cases} 3eV, \ 0 \le r < 0.25\text{Å} \\ 0.265eV, \ 0.25\text{Å} \le r < 3.5\text{Å} \\ 0.25eV, \ 3.5\text{Å} \le r \end{cases}$$

The quantum transmission probability T can then be calculated. The ratio of transmission probability ( $T_{13}$ ) of  $^{13}CO_2$  to that ( $T_{12}$ ) of  $^{12}CO_2$  is calculated to be 0.70.

After the electron is excited to the LUMO of the adsorbed CO2 molecule, the molecule may be dissociated to CO in the life time of an electron in the LUMO state. The longer the lifetime of the electron in the LUMO, the higher the probability for dissociation. If we do not consider the interaction with the radiation field, the energy of the CO2 system consists of electronic energy,  $E_{electron} = E_{LUMO}$ ; vibrational energy,  $E_{vibrational}$ ; a possible translational energy of the molecule, K; and the interaction of electron with the CO<sub>2</sub> molecule ion and the CoO solid,  $H^{\prime}$  ; i.e.  $E=E_{electron}+E_{vibrational}+K+H^{\prime}.$  In the simple adiabatic model, we may neglect H'. The lifetime  $\Delta t = \frac{h}{2\Delta E}$  is estimated with the energy-time uncertainty principle [26], where  $\Delta E$  is the energy uncertainty of the excited system. When  $E_{electron} = E_{LUMO}$  in the first excited state and  $E_{vibrational}$  is in the ground state,  $E_{electron} + E_{vibrational}$  do not contribute to  $\Delta E$  in this simple adiabatic model. If there were not any translational motion of the  $CO_2$  molecule,  $\Delta E$  would be zero and  $\Delta t$ would be infinitely long. However, as the adsorbed molecule may migrate on the solid surface [27], this uncertainty may contribute to  $\Delta E$ and  $\Delta t$  is no longer infinitely long. We may estimate  $\Delta E$  with the kinetic energy of the carbon atom, i.e.  $\Delta E = K = \frac{1}{2}mv^2$ , where m is the mass of the carbon atom and  $\nu$  is its average migration speed. The speed may mainly be related to molecular configuration of the surface [27]. Since the mass of the carbon-12 atom (m<sub>12</sub>) is different from that of carbon-13 (m<sub>12</sub>), the lifetime of an electron in their LUMO states is different. The ratio of the life time of  $^{12}\text{CO}_2$  ( $\Delta t_{12}$ ) to that of  $^{13}\text{CO}_2$  ( $\Delta t_{13}$ ) is estimated by

$$\frac{\Delta t_{12}}{\Delta t_{13}} = \frac{m_{13}}{m_{12}} \tag{3}$$

where  $m_{13}=13$  Da,  $m_{12}=12$  Da. Therefore, the ratio of the lifetime of carbon-13 to that of carbon-12 is calculated to be 0.92. This may also contribute to the carbon isotope effect in the artificial photosynthesis reaction in addition the quantum tunneling. For the experiment with an equal molar ratio of  $^{12}\text{CO}_2$  and  $^{13}\text{CO}_2$  as the reagents, we are able to estimate the ratio of  $^{13}\text{C}$  to  $^{12}\text{C}$  in the hydrocarbons to be  $\frac{\Delta_{13}}{\Delta_{12}} \cdot \frac{\eta_{13}}{\eta_{12}} = 0.92 \times 0.70 = 0.64$ , which is fitted to the ratios of experiment (b) as shown in Table 1.

From the fact that the dissociation of <sup>12</sup>CO<sub>2</sub> is easier than that of <sup>13</sup>CO<sub>2</sub>, we know that there is more dissociated carbon dioxide in

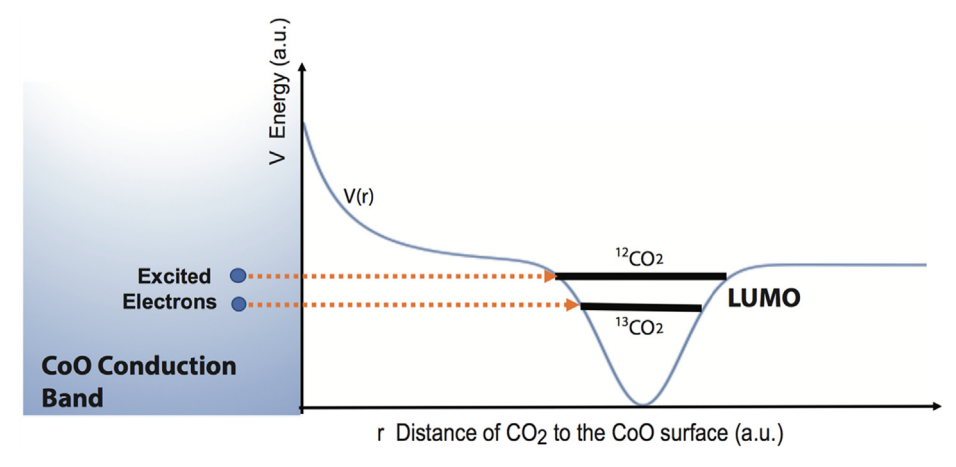


Fig. 4. Cartoon of electron potential barrier of CO<sub>2</sub> absorbed on to CoO surface. The excited electrons are tunneling to the CO<sub>2</sub>'s LUMO levels with vibrational energies.

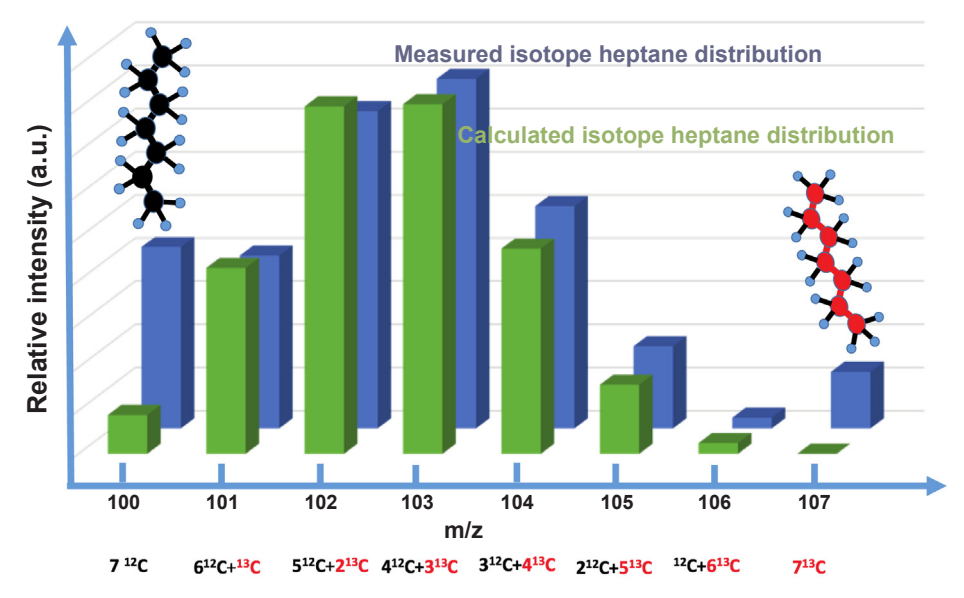


Fig. 5. Comparison of the calculated isotope heptane distribution and the measured isotope heptane distribution.

experiment (a). Therefore, we are able to understand that the longest hydrocarbon in experiment (a) is longer than that in experiments (b) and (c) because the higher the concentration of disassociated carbon dioxide, the higher the probability to form a longer hydrocarbon chain.

### 3.3. Anomalous isotope distribution in the hydrocarbon chains

If we suppose that during the formation of the hydrocarbons, the carbon atoms are selected randomly, then a simple method of combination can be used to predict the pattern of the mass spectra. For instance, from the mass spectrum of heptane in experiment (a), the ratio of  $^{13}\mathrm{C}$  to  $^{12}\mathrm{C}$  is 0.65. For convenience, we assume that there are 100  $^{12}\mathrm{C}$ atoms and 65 <sup>13</sup>C atoms, so the probability of forming a heptane chain with all 7 carbon atoms being  $^{12}$ C is  $\frac{C_{100}^2}{C_{165}^2}$  = 0.028. The probability of forming a heptane chain with 6  $^{12}$ C atoms and 1  $^{13}$ C atom is  $\frac{C_{100}^6C_{65}^6}{c^7}=0.133$ , etc. Therefore, a series of theoretical M to M + n molecular ion peaks is obtained. As shown in Fig. 6, the calculated isotope heptane distribution (green color bars) differs from the measured isotope heptane distribution (blue color bars). However, it is observed that the two distributions match well except for the ones with all 7 carbon atoms being 12C and 13C; this indicates that the same carbon isotope atoms have a higher probability to bond together to form the hydrocarbon chain. The quantum mechanical resonant-tunneling effect may explain this anomalous phenomenon.

In quantum mechanics, when a particle with a certain energy travels towards a potential barrier that has a greater energy, there is a small probability that this particle can tunnel to the other side. This phenomenon is called quantum tunneling, which cannot be adequately

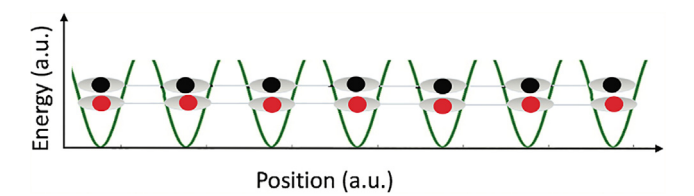


**Fig. 6.** The energy level of electrons (silver colored) of carbon-12 atoms (black dots) and that of electrons (silver colored) of carbon-13 atoms (red dots), when vibrational energy is taken into account in the potential energy wells (green colored). The same isotope atoms have strong interaction due to the resonantly tunneling effect. (For interpretation of the references to color in this figure legend, the reader is referred to the web version of this article.)

explained by classical mechanics. It has been shown that the tunneling of electrons may lead to the anomalous isotope effects in chemical reactions [28–30].

Resonant tunneling also occurs in potential profiles with more than two barriers. During the process of the formation of the hydrocarbon chains in the artificial photosynthesis, resonant tunneling plays an important role because the same carbon isotope atoms have a higher probability to bond together.

As shown in Fig. 6, the black dots represent the energy levels of carbon-12, and the red dots represent the energy levels of carbon-13. Since the same carbon isotopes have the same energy levels, the probability of quantum tunneling of electrons between the same carbon isotopes is higher than that between different carbon isotopes. Therefore, it is observed that there are more hydrocarbon chains with pure carbon-12 atoms and pure carbon-13 atoms produced than expected.

To better explain that the measured abundances differ from the predicted abundances as shown in Fig. 5, we apply the Bayesian statistics technique to quantitively analyze the tendency that the same isotope carbon atoms like to join together. Considering that the hydrocarbons may form through two paths: one classical and the other quantum. The calculated distribution in Fig. 5 is for a classical mechanics model where we have not considered any preference. Let R(r)be the bonding preference between two <sup>12</sup>C (<sup>13</sup>C) atoms. If there is a group of  $n^{12}$ C ( $^{13}$ C) atoms, the bonding preference is  $R^{n-1}$  ( $r^{n-1}$ ), where n is an integer larger than 1 and smaller or equal to the number of carbon atoms in the hydrocarbons. Let D (d) be the bonding preference between a single  $^{13}$ C ( $^{12}$ C) atom and a group of n  $^{12}$ C (n  $^{13}$ C) atoms. Let N be that between a group of  $n^{12}$ C atoms and a group of  $n^{13}$ C atoms. When the preference parameter is larger than 1, the atoms like to join together. When the parameter is smaller than 1, they dislike to join together. When the parameter is equal to 1, the same as classical bonding, they have no preference. The likelihood for each isotope heptane is given in Table 2. Taking the likelihoods and considering the calculated distribution in Fig. 5 as the prior, we can get the posterior which is the distribution of isotope heptane formed via the quantum mechanical effect. If we suppose there is Q% of the heptane molecules formed via the quantum mechanical effect, we can fit the calculation  $prior \cdot (100 - Q)\% + posterior \cdot Q\%$  to the experimental distribution. As shown in Fig. 7, the calculation with the quantum mechanical effect fits the experimental abundances very well. We found that Q = 30, i.e. about 30% of the heptane is formed through the quantum mechanical effect. R and r are 8 and 12, respectively; which shows that same isotope carbon atoms obviously prefer to join together. D, d and N are 0.5,

Table 2

Likelihood for isotope heptane quantum mechanical formation. R, r, D, d and N are preference parameters, please read the context for their definitions.

	7 <sup>12</sup> C	$6^{12}C + {}^{13}C$	$5^{12}C + 2^{13}C$	$4^{12}C + 3^{13}C$	$3^{12}C + 4^{13}C$	$2^{12}C + 5^{13}C$	$^{12}\text{C} + 6^{13}\text{C}$	7 <sup>13</sup> C
Likelihood	$R^6$	$R^5D$	$R^4rN$	$R^3r^2N$	$R^2r^3N$	$Rr^4N$	$r^5d$	$r^6$

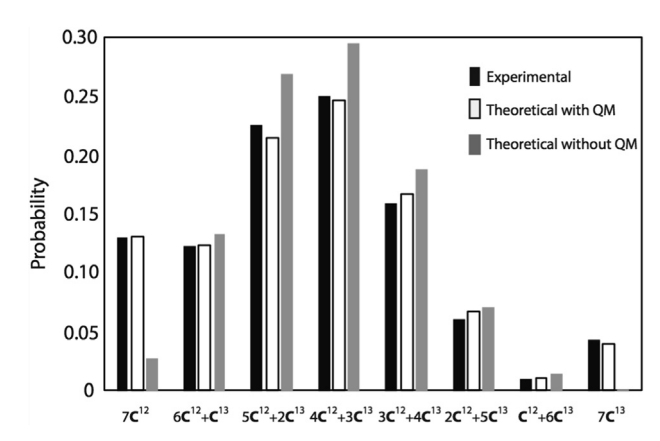


**Fig. 7.** The calculated isotope heptane distributions with and without considering the quantum mechanical effect, and the experimental distribution.

0.0, and 0.1, respectively, which shows that different isotope carbon atoms obviously do not like to join together. A single  $^{13}\mathrm{C}$  atom can join a group of n  $^{12}\mathrm{C}$  but at low preference, D = 0.5; a group of n  $^{12}\mathrm{C}$  and a group of n  $^{12}\mathrm{C}$  can join together but at much lower preference N = 0.1; while a single  $^{12}\mathrm{C}$  atom cannot join a group of n  $^{13}\mathrm{C}$  because d = 0. The fitting also shows that in the pure  $^{12}\mathrm{C}$  heptane, about 30% are formed quantum mechanically, while in the pure  $^{13}\mathrm{C}$  heptane, more than 90% are formed quantum mechanically.

The resonant quantum tunneling model also explains the observed ratio of <sup>13</sup>C to <sup>12</sup>C for experiments (a) and (c) in Fig. 3 and Table 1. Fig. 3a shows the relative amounts of  $7^{12}$ C and  $6^{12}$ C +  $^{13}$ C. Due to the resonant tunneling effect,  $6^{12}C + ^{13}C$  is most likely formed from a single <sup>13</sup>C joining a 6<sup>12</sup>C group, in which the six <sup>12</sup>C atoms have been interacting via the resonant tunneling effect. By taking the molecular vibration energy into account, we know that the ground state energy level of the single <sup>13</sup>C is lower than that of 6<sup>12</sup>C (or n<sup>12</sup>C) group. The <sup>13</sup>C, due to its electrons in the excited state, resonantly interacts with the 612C group (or n<sup>2</sup>C). This makes the <sup>13</sup>C joining the 6<sup>12</sup>C group possible in agreement with D = 0.5 in the above Bayesian analysis although the dissociation rate of <sup>13</sup>CO<sub>2</sub> of about 20% is less than that of <sup>12</sup>CO<sub>2</sub>. As for the ratio of <sup>13</sup>C to <sup>12</sup>C for experiment (c), the carbon-12 related molecular MS signal is too weak to find a reliable ratio of 13C to 12C. Similarly, due to the resonant tunneling effect,  $^{12}C + 6^{13}C$  is most likely formed from a single <sup>12</sup>C joining a 6<sup>13</sup>C group in which the six <sup>13</sup>C atoms have been interacting via the resonant tunneling effect, but the ground state energy level of a single  $^{12}\mathrm{C}$  is higher than that of  $6^{13}\mathrm{C}$  (or n<sup>13</sup>C) group, which may make the <sup>12</sup>C joining the 6<sup>13</sup>C (or n<sup>13</sup>C) group very difficult without resonant quantum tunneling, this is in agreement with d = 0 in the above Bayesian analysis. Thus, the amount of  $^{12}\mathrm{C}\,+\,\mathrm{n}^{13}\mathrm{C}$  is too small to be detected. However, additional modelling is needed in the future to explain all the observed behavior in the present experiments.

# 4. Summary

 $^{12}\text{C}/^{13}\text{C}$  competition experiments using an equal molar ratio of  $^{12}\text{CO}_2$  and  $^{13}\text{CO}_2$  as the reagents were conducted to study the carbon isotope effect. GC–MS was used in the isotope analysis because it is adequate for measuring the isotope ratios of  $^{12}\text{C}$  and  $^{13}\text{C}$  and because the mass spectra reveal the distribution of the  $^{12}\text{C}$  and  $^{13}\text{C}$  in the synthesized hydrocarbons. Two anomalous isotope effects were found: 1)

the dissociation of  $^{12}\text{CO}_2$  is easier than that of  $^{13}\text{CO}_2$  and 2) the same carbon isotope atoms have a relatively higher probability to bond together to form the hydrocarbon chain than do different ones.

During the process of the hot-electrons injecting into the conduction band of CoO and the subsequent quantum tunneling to the LUMO energy levels of  $\rm CO_2$  molecules, a simplified two-step potential barrier for the quantum tunneling was used to explain the first carbon isotope effect.

A conceptual quantum resonant tunneling model is used to explain the second carbon isotope effect. Since the same carbon isotopes have the same energy levels, the probability of quantum tunneling of the electrons between the same carbon isotopes is higher than the probability of quantum tunneling of electrons between different carbon isotopes. Therefore, it is observed that hydrocarbon chains with pure carbon-12 atoms or pure carbon-13 atoms are more abundant than expected.

#### **Author contributions**

M.Z. and M.S. conceived the idea for the project. M.Z. prepared samples and performed the hydrocarbon synthesis experiments. M.Z., Z.K. and Z.W. analyzed the synthesized products. M.Z., Z.K., Z.W. and MS. discussed the results, analyzed the data, and drafted the manuscript. M.S. finalized the manuscript.

#### **Declaration of Competing Interest**

The authors declare that they have no known competing financial interests or personal relationships that could have appeared to influence the work reported in this paper.

### Acknowledgements

We thank Dr. C. Wang, Dr. H. Ren, and Dr. M. Jayamanna for experimental assistance; and Dr. D. Ryan, and Dr. M. Ruths for helpful discussions. This research was supported by the National Science Foundation (CHE-1836540 and CMMI-1161475) and Department of Energy.

#### References

- [1] M. Pessarakli, Handbook of photosynthesis, CRC Press2016.
- [2] C. Wang, M. Shen, H. Huo, H. Ren, F. Yan, M. Johnson, Erratum: "Nature-like photosynthesis of water and carbon dioxide with femtosecond laser induced selfassembled metal nanostructures", Int. J. Mod Phys. B 28 (2014).
- [3] C. Wang, M. Shen, H. Huo, H. Ren, M. Johnson, Using metal nanostructures to form hydrocarbons from carbon dioxide, water and sunlight, AIP Adv. 1 (2011) 042124.
- 4] C.G. Visconti, L. Lietti, E. Tronconi, P. Forzatti, R. Zennaro, E. Finocchio, Fischer-Tropsch synthesis on a Co/Al<sub>2</sub>O<sub>3</sub> catalyst with CO<sub>2</sub> containing syngas, Appl. Catal. A 355 (2009) 61–68.
- [5] M.K. Gnanamani, W.D. Shafer, D.E. Sparks, B.H. Davis, Fischer-tropsch synthesis: effect of CO<sub>2</sub> containing syngas over Pt promoted Co/γ-Al<sub>2</sub>O<sub>3</sub> and K-promoted Fe catalysts, Catal. Commun. 12 (2011) 936–939.
- [6] Z. Kan, Q. Zhang, H. Ren, M. Shen, Femtosecond laser induced formation of graphene nanostructures in water and their field emission properties, Mater. Res. Express 6 (2019) 085016.
- [7] Z. Kan, Q. Zhu, H. Ren, M. Shen, Femtosecond laser-induced thermal transport in silicon with liquid cooling bath, Materials 12 (2019) 2043.
- [8] Q. Zhu, C. Wang, H. Ren, M. Zeng, Z. Kan, Z. Wang, M. Shen, Conversion of water and carbon dioxide into methanol with solar energy on Au/Co nanostructured surfaces, Mater. Res. Express 7 (2020) 35014.
- [9] C. Wang, H. Ren, M. Zeng, Q. Zhu, Q. Zhang, Z. Kan, Z. Wang, M. Shen, M.J.T. Acharige, M. Ruths, D.K. Ryan, G. Li, G. Kolesov, E. Kaxiras, E. Mazur, Lowcost visible-light photosynthesis of water and adsorbed carbon dioxide into long-

- chain hydrocarbons, Chem. Phys. Lett. 739 (2020) 136985.
- [10] K.B. Wiberg, The deuterium isotope effect, J. Chem. Rev. 55 (1955) 713-743.
- [11] F. Westheimer, The magnitude of the primary kinetic isotope effect for compounds of hydrogen and deuterium, Chem. Rev. 61 (1961) 265–273.
- [12] P. Vidmar, A. Lesar, I. Kobal, J. Koller, Theoretical interpretation of kinetic isotope effects for the reaction of CO<sub>2</sub> on a Mg surface, J. Phys. Chem. 100 (1996) 5781–5787.
- [13] T. Giagou, M.P. Meyer, Kinetic isotope effects in asymmetric reactions, Chem.–A European J. 16 (2010) 10616–10628.
- [14] K.C. Westaway, Y.-R. Fang, S. MacMillar, O. Matsson, R.A. Poirier, S.M. Islam, Determining the transition-state structure for different SN2 reactions using experimental nucleophile carbon and secondary α-deuterium kinetic isotope effects and theory, J. Phys. Chem. A 112 (2008) 10264–10273.
- [15] J.E. Baldwin, S.S. Gallagher, P.A. Leber, A.S. Raghavan, R. Shukla, Deuterium kinetic isotope effects and mechanism of the thermal isomerization of bicyclo [4.2. 0] oct-7-ene to 1, 3-cyclooctadiene, J. Organic Chem. 69 (2004) 7212–7219.
- [16] G.D. Farquhar, J.R. Ehleringer, K.T. Hubick, Carbon isotope discrimination and photosynthesis, Annu. Rev. Plant Physiol. Plant Mol. Biol. 40 (1989) 503–537.
- [17] C. Handbook, Handbook of chemistry and physics, Boca Raton, FL, USA: CRC Press LLC, 2002.
- [18] F.W. McLafferty, F. Tureček, F. Tureček, Interpretation of mass spectra, University science books1993.
- [19] J.T. Watson, O.D. Sparkman, Introduction to mass spectrometry: instrumentation, applications, and strategies for data interpretation, John Wiley & Sons, 2007.

- [20] A. Nitzan, Chemical dynamics in condensed phases: relaxation, transfer and reactions in condensed molecular systems, Oxford university press, 2006.
- [21] B.W. Pfennig, Principles of inorganic chemistry, John Wiley & Sons, 2015.
- [22] W.A. Goddard III, D. Brenner, S.E. Lyshevski, G.J. Iafrate, Handbook of nanoscience, engineering, and technology, CRC press, 2012.
- [23] K.S.H. Ishi, E. Ito, K. Seki, Energy level alignment and interfacial electronic structures at organic/metal and organic/organic interfaces, Adv. Mater. 11 (1999) 605–625.
- [24] A.K.D. Cahen, Electron energetics at surfaces and interfaces: concepts and experiments, Adv. Mater. 15 (2003) 271–277.
- [25] M. Zhou, B. Liang, L. Andrews, Infrared spectra of OMCO (M= Cr Ni), OMCO-(M= Cr - Cu), and MCO2-(M= Co - Cu) in Solid Argon, J. Phys. Chem. A 103 (1999) 2013–2023.
- [26] R.D. Knigh, Physics for Scientists and Engineers: A Strategic Approach with Modern Physics (2007).
- [27] I.A.W.F.L. Joos, S. Cottenier, E.J.M. Hensen, M. Waroquier, V. van Speybroeck, R.A. van Santen, Reactivity of CO on carbon-covered cobalt surfaces in Fischer-Tropsch synthesis, J. Phys. Chem. C 118 (2014) 5317–5327.
- [28] V. Goldanskii, Chemical reactions at very low temperatures, Annu. Rev. Phys. Chem. 27 (1976) 85–126.
- [29] R. Bell, The Tunnel Effect in Chemistry, New York City, Chapman Hall, 1980.
- [30] R. Compton, Electron tunneling in chemistry: chemical reactions over large distances. comprehensive chemical kinetics, Elsevier Science & Technology 30 (1989).